Hydrophobic Interactions in the Hinge Domain of DNA Polymerase β Are Important but Not Sufficient for Maintaining Fidelity of DNA Synthesis†

Patricia L. Opresko,‡,§ Ross Shiman,‖ and Kristin A. Eckert*,‡

Department of Biochemistry and Molecular Biology and The Jake Gittlen Cancer Research Institute, Pennsylvania State University College of Medicine, M. S. Hershey Medical Center, P.O. Box 850, Hershey, Pennsylvania 17033, and Department of Chemistry, Johns Hopkins University, 3400 North Charles Street, Baltimore, Maryland 21218

Received March 28, 2000; Revised Manuscript Received July 13, 2000

ABSTRACT: We previously described a general mutator form of mammalian DNA polymerase β containing a cysteine substitution for tyrosine 265. Residue 265 localizes to a hydrophobic hinge region predicted to mediate a polymerase conformational change that may aid in nucleotide selectivity. In this study we tested the hypothesis that van der Waals and hydrophobic contacts between Y265 and neighboring residues are important for DNA synthesis fidelity and catalysis, by altering interactions in the hinge domain via substitution at position 265. Consistent with the importance of hydrophobic interactions, we found that phenylalanine, leucine, and tryptophan substitutions did not alter significantly the steady-state catalytic efficiency of DNA synthesis, relative to wild type, while the polar serine substitution decreased catalytic efficiency 6-fold. However, we found that all substitutions other than phenylalanine increased the error frequency, relative to wild type, in the order serine > tryptophan = leucine. Therefore, maintenance of the hydrophobicity of residue 265 was not sufficient for maintaining fidelity of DNA synthesis. We conclude that while hydrophobic interactions in the hinge domain are important for fidelity, additional factors such as electrostatic and van der Waals interactions contributed by the tyrosine 265 aromatic ring are required to retain wild-type fidelity.

The recently solved binary and ternary X-ray crystal structures of various DNA polymerase I family members and of DNA polymerase β (pol β)[1] have identified common structural features that may function in nucleotide discrimination during DNA synthesis (reviewed in ref *1*). Binding of the dNTP induces a conformational change whereby a movable subdomain closes over the substrate, allowing residues in this subdomain to contact the newly formed base pair. This conformational change assembles the active site and is predicted to select for the correct geometry of Watson−Crick base pairs by an induced fit mechanism (reviewed in refs *1* and *2*). In addition, polymerase side chains form hydrogen bonds with the O^2 atoms of pyrimidines and N3 atoms of purines in the minor groove of Watson−Crick base pairs at the active site. These atoms are shifted out of position in non-Watson−Crick base pairs such that hydrogen bonding with polymerase side chains is predicted to be lost (reviewed in ref *1*). Structure−function analyses of polymerase mutants are being used to test the importance of polymerase contacts with substrate and are offering insights into the mechanisms of polymerase nucleotide discrimination.

Specific pol β intraprotein interactions also function in DNA synthesis fidelity, as indicated by pol β mutators Y265C,H which are altered in residues not predicted to contact substrate (*3*). We previously determined Y265 functions in a general discrimination mechanism, since the pol β mutator Y265C displayed a nearly equivalent increase in both misalignment-initiated frame-shift errors and misincorporation-initiated base substitution errors, relative to wild type (*4*). This alteration also resulted in a nearly 20-fold decrease in the steady-state catalytic rate constant (*3*). Residue Y265 localizes to a hinge region between two subdomains that is predicted to mediate the polymerase conformational change described above (*5*). This conformational change may be similar to the rate-limiting polymerase conformational change that occurs prior to catalysis (*6*, *7*) and is predicted to result from changes in the torsion angles of amino acids 263, 264, and 265 which form a hinge (*8*). This hinge is lined on the inside (closest to the active site) with hydrophobic residues leucine 194, isoleucine 260, phenylalanine 272, and tyrosine 296 and on the outside with residues isoleucine 174, threonine 196, and valine 269, so that an equal number of favorable hydrophobic interactions occur in the open and closed conformations (*8*) (Figure 1). We predicted that the introduction of a more polar side chain (cysteine) compromised proper hinge function by disrupting hydrophobic and van der Waals interactions in this region. A defect in the conformational change due to an altered hinge region of pol β Y265C was predicted to loosen the constraints normally imposed on the newly formed base pair (*4*).

To examine this model in more detail, we have altered interactions in the hinge domain by substituting various

† This research was supported by the American Cancer Society (Grant RPG-95-075).

* To whom correspondence should be addressed. Tel: 717-531-4065. Fax: 717-531-5634.

‡ Pennsylvania State University College of Medicine.

§ Present address: Laboratory of Molecular Genetics, National Institute of Aging, 5600 Nathan Shock Drive, Baltimore, MD 21224.

‖ Johns Hopkins University.

[1] Abbreviations: pol, polymerase; β-wt, wild-type DNA polymerase β; HSV-*tk*, herpes simplex virus type 1 thymidine kinase.

10.1021/bi000698t CCC: $19.00
Published on Web 08/18/2000

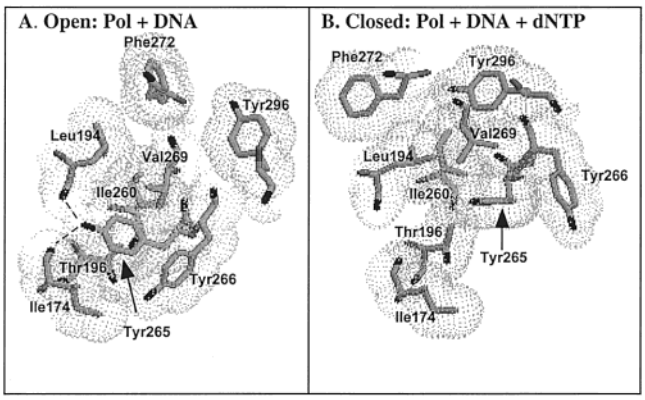

FIGURE 1: Amino acid residues interacting in the hinge domain of pol β-wt binary and ternary crystal structures. The hydrophobic hinge region includes residues Ile174, Leu194, Thr196, Ile260, Phe272, Tyr265, Tyr266, Val269, and Tyr296. (A) Residues in the open binary conformation. (B) Residues in the closed ternary conformation. Pictures were generated using RasMol software and X-ray crystal structure coordinates published by Sawaya et al. (*5*).

amino acids at position 265. Amino acids for substitution were selected on the basis of their reported van der Waals volume (*9*) and side chain hydropathy index [free energy of transfer from water to a nonpolar sovlent (*10*)]. Substitutions of phenylalanine and leucine were performed in order to maintain the van der Waals volume and hydrophobicity of residue 265. In contrast, a serine substitution was constructed to measure the effects of a polar residue in the hinge region. Finally, tryptophan was substituted to determine whether introduction of a larger residue, while maintaining hydrophobicity and aromaticity, would disrupt critical interactions in the hinge. We observed that hydrophobic contacts were required for achieving a catalytic efficiency as high as wild type but were not sufficient for maintaining fidelity.

MATERIALS AND METHODS

Reagents. All restriction enzymes and T4 polynucleotide kinase were supplied by Gibco BRL Life Technologies (Gaithersburg, MD) or New England BioLabs (Beverly, MA) and were used according to the manufacturer's protocol. Bovine serum albumin (BSA) was supplied by Gibco BRL.

Generation of Polymerase β Y265 Substitution Variants. The pET-28a(+) expression vector (Novagen, Madison, WI) containing rat pol β cDNAs (wt, Y265F, Y265C) cloned 3′ to a hexahistidine tag was supplied by Joann Sweasy (Yale University). We used oligonucleotide site-directed mutagenesis to generate the Y265L, Y265S, and Y265W substitutions (*11*). The oligonucleotides (Biosynthesis, Lewisville, TX) containing the appropriate 265 codon substitutions also introduced a unique PinAI site 21 bases downstream via silent base substitutions. The PinAI site, which distinguishes the newly created mutant from the original wild-type vectors, was used to identify mutants and to eliminate residual contaminating pol β-wt plasmid by subcloning. The final pol β sequence for each construct was confirmed by DNA sequence analysis (Pennsylvania State College of Medicine Macromolecular Core Facility).

Purification of Polymerase β 265 Substitution Variants. We purified the hexahistidine fusion proteins of the wild-type pol β and 265 substitutions as previously described with some modification (*12*, *13*). Pol β expression was induced with 2 mM IPTG for 3 h at 30 °C. Prepared cell extracts were mixed with Ni−NTA resin (Qiagen, Valencia, CA) according to the manufacturer's protocol prior to being loadied on a column. After washing and protein elution, fractions containing protein were exchanged into 50 mM Tris-HCl, pH 7.5, 1 mM EDTA, 100 mM NaCl, and 15% glycerol buffer using a Centricon-30 device (Millipore, Bedford, MA). The sample was loaded on a column containing single-stranded DNA−cellulose (Sigma) and washed with 250 mM NaCl, and protein was eluted with 500 mM NaCl. Protein-containing fractions were concentrated and exchanged into storage buffer. Protein samples were determined to be 97−99% homogeneous on the basis of densitometric analysis of Coomassie-stained SDS−polyacrylamide gels (data not shown). Western blot analysis (ECL kit, Amersham Pharmacia) was performed with a polyclonal antibody against pol β (Joann Sweasy, Yale University) and confirmed the identity of the proteins.

Kinetic Analyses. A gapped DNA primer template containing five adenosine residues was constructed by annealing three oligonucleotides as follows:

```
                3'TCGTCAACGCACCAGCAAAAAGCGTAGGGCACTCCT5' (template)

(priming) 5'AGCAGTTGCGTGGTCG          CGCATCCCGTGAGGA3' (downstream)

                  3'OH      5'(PO4 or OH)
```

The downstream oligonucleotide was phosphorylated with T4 polynucleotide kinase according to the manufacturer's protocol and purified using Microcon-3 ultrafiltration devices (Amicon Inc., Beverly, MA) and G-25 Sephadex Quick Spin columns (Boehringer Mannheim Corp., Indianapolis, IN). The concentration was determined by spectrophotometry. Hybridization reactions contained a 1:1:1.2 ratio of template, priming, and downstream oligonucleotides. Reactions were incubated at 70 °C and allowed to cool to room temperature.

DNA polymerase reactions contained 300 nM gapped DNA, 50 mM Tris-HCl, pH 8.5, 50 mM NaCl, 200 μg/mL bovine serum albumin, 1 mM dithiothreitol, 2 mM $MnCl_2$, 20−60 nM DNA polymerases, 2−200 μM TTP, and 0.11−0.22 μM [α-^{32}P]TTP (3000 Ci/mmol) (Amersham Pharamacia). Reactions were preincubated at 37 °C for 3 min and initiated with the addition of polymerase. Aliquots were removed at 15, 30, 60, 120, and 240 s and quenched in a 20× volume of 25 mM EDTA on ice. Incorporation of [α-^{32}P]TTP was measured by a dot blot procedure (*14*), with some modification. The full volume (100 μL) of the quenched reaction aliquots was loaded onto a 96-well dot blot apparatus (Schleicher & Schuell, Keene, NH) that was fitted with a NA-45 DEAE membrane (Schleicher & Schuell). The wells were vacuum washed with 500 μL of 0.3 M ammonium formate, pH 8.0, followed by membrane removal and additional washing with 0.3 M ammonium formate, pH 8.0, while shaking. The membrane was allowed to dry and exposed to a Molecular Dynamics Phosphorimager screen (Sunnyvale, CA). To determine the total TTP in each reaction, Mn·TTP/Mn·[α-^{32}P]TTP stocks were spotted on a separate piece of membrane and exposed to the Phosphorimager screen. Quantitation was performed using a Molecular Dynamics Phosphorimager.

To determine the K_m(TTP) for five nucleotide gap filling, the initial velocity (v_0) was calculated from the reaction

Scheme 1

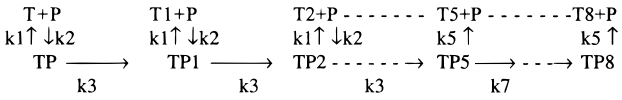

progress curves. For all of the pol β 265 substitutions analyzed and for pol β-wt with both Mg^{2+} and Mn^{2+}, reaction plots of picomoles of TMP incorporated versus time followed a first-order decay curve and could be fit to the equation: $y = c(1 - e^{-bt})$ where t = time. Initial velocities were obtained from the first derivative of this equation, $v_0 = dy/dt = cb(e^{-bt})$ at $t = 0$ s. Plots of initial velocity versus TTP concentration were hyperbolic and were fit to the Michaelis−Menten equation using KaleidaGraph (Synergy Software, Reading, PA), from which the V_{max} and K_m(TTP) values were obtained. The k_{cat} values were calculated by dividing V_{max} by the initial polymerase concentrations.

Primer Extension Analysis of Kinetic Reactions. The five nucleotide gap kinetic template (5′PO_4) was constructed as above, except the priming oligonucleotide was radioactively labeled at the 5′-end using [γ-^{32}P]ATP (5000 Ci/mmol) (Amersham Pharmacia) with T4 polynucleotide kinase according to the manufacturer's protocol. Control templates were constructed as above, except the downstream primer was nonphosphorylated (5′OH). Reactions contained 100 nM 5′PO_4 or 5′OH gapped template, 6.7 nM pol β-wt, 100 μM TTP, and either 2 mM $MnCl_2$ or 10 mM $MgCl_2$ in the same buffer and conditions as in the dot blot assay. Reactions were quenched in stop dye, and 20 fmol of DNA from each time point was loaded on a 16% denaturing polyacrylamide gel. Products were quantitated using a Molecular Dynamics Phosphorimager. A control for the percent hybridization of gap template was performed for each preparation using Klenow polymerase as described previously (*4*). The degree of DNA synthesis in each reaction was defined as the percent of primers extended. The distribution of products for each reaction was defined as the percent of primers extended each length as a function of total primer molecules in the reaction.

Rate constants to describe five nucleotide gap filling under various experimental conditions were calculated from the model in Scheme 1 by computer simulation using the program Madonna (www.berkeleymadonna.com).

The model shows that the polymerase (P) binds to free template (T, T1, ..., T4) and then either dissociates (k_1, k_5) or catalyzes the extension (k_3, k_7) of the primer by one nucleotide. The experimental results (see Figure 3) indicate that either the dissociation rate, the extension rate, or both change after the primer has been extended five nucleotides; consequently, the rate constants in the model are allowed to change at that point. Since the gapped template is five nucleotides long, the polymerase is assumed to either not bind or bind extremely poorly to templates with five or more added nucleotides (i.e., for $i \geq 5$ on Ti). To keep the model as simple as possible, a separate step for TTP binding was omitted (its concentration did not change during the reaction), and rate constants for polymerase association, dissociation, and extension (k_1, k_2, k_3) were assumed to be unaffected by template extension until after addition of five nucleotides. The apparent rate of polymerase activity loss has been incorporated into the calculations either by assuming the enzyme loses activity and dissociates from the gapped template, freeing substrate for attack by another enzyme, or by assuming the enzyme stalls and is trapped on the gapped template, thereby sequestering substrate. Equivalent results are obtained in the two cases.

Herpes Simplex Virus Type 1 Thymidine Kinase (HSV-tk) Forward Mutation Assay. Pol β-wt and Y265 substitutions were used in the previously described HSV-*tk* forward mutational assay (*15*) to compare in vitro mutation frequencies. DNA synthesis reactions (50 μL) contained 2 pmol of template (oligonucleotide-primed M13tk3.5 single-stranded DNA containing the HSV-*tk* gene), 10 mM $MgCl_2$ or 2 mM $MnCl_2$, and 1 mM dNTPs in reaction buffer (as above). Reactions were initiated by addition of either 25 pmol of pol β-wt, 25 pmol of Y265F, 25 pmol of Y265W, 150 pmol of Y265L, 300 pmol of Y265C, or 450 pmol of Y265S. The amounts of enzyme required to achieve nearly equivalent amounts of in vitro DNA synthesis for the various polymerases were determined empirically. Parallel reactions supplemented with 5 μCi of [α-^{32}P]dCTP (3000 Ci/mmol) (Amersham Pharmacia) were performed to determine the efficiency of DNA synthesis (*15*), with the modification that approximately 50 fmol of ^{32}P 5′-end-labeled 15-mer oligonucleotides was added to the reactions after termination. This DNA served as an internal loading standard for subsequent quantitation of synthesis products by Phosphorimager analysis (Molecular Dynamics).

Synthesis products were analyzed for the presence of inactivating HSV-*tk* mutations as previously described (*15*). Briefly, products were digested with restriction enzymes, and the resulting 203 base pair fragments were hybridized to gapped duplex molecules bearing a functional chloramphenicol (Cm) resistance gene on the product-containing strand. Resulting plasmids were electroporated into *Escherichia coli* strain FT334 (*recA*13, *tdk*). Bacteria were plated in the presence of Cm to select for progeny of the product-containing strand and in the presence of 5-fluoro-2′-deoxyuridine (FUdR) to select for inactivating HSV-*tk* gene mutations. The observed HSV-*tk* mutation frequencies were calculated as the number of Cm- and FUdR-resistant colonies divided by the total Cm-resistant colonies. Error specificities were determined by dideoxy DNA sequence analysis of the *Mlu*I−*Eco*RV target region of independent HSV-*tk* mutants, using Sequenase 2.0 according to the manufacturer's protocol (Amersham Pharmacia). The observed mutation frequencies (MF_{obs}) were adjusted for any preexisting, inactivating HSV-*tk* mutations (*4*) and for the existence of multiple errors. An estimated polymerase error frequency (EF_{est}) was determined using the formula:

$$MF^{obs} = \sum_{n=1}^{4}(1/n)(\text{mutants with } n \text{ errors/total sequenced mutants})(EF_{est})$$

where n represents the number of independent, detectable polymerase errors observed in the 203 base pair target sequence for each HSV-*tk* mutant characterized. DNA sequence changes are considered independent polymerase errors if the mutations occur at sites greater than 15 nucleotides apart or if evidence exists for either error occurring alone. A DNA sequence change is defined as a detectable polymerase error when the alteration results in

an FUdR-resistant phenotype in the absence of other mutations. Detectable errors include all frame shifts and previously observed single base substitutions within the HSV-*tk* database of over 1000 sequenced mutants (K. Eckert, unpublished data). The EF_{est} was used to calculate the frequency of specific error types. Differences in proportions of specific error types were analyzed using Fisher's exact test (two-tailed) (*16*).

RESULTS

To identify the structural features of residue 265 that are important for pol β catalytic efficiency and DNA synthesis fidelity, we compared residues that vary in van der Waals volume, hydrophobicity, and aromaticity (*9*, *10*): Y265 (wild type), Y265F, Y265L, Y265W, and Y265S.

Steady-State Kinetic Analysis of Gap Filling. To compare the catalytic efficiency of the Y265 substitutions, we performed steady-state kinetic analyses using a five nucleotide gapped DNA substrate that contained a poly(dA) template sequence. Under the steady-state conditions of this assay, Mg^{2+} failed to support saturation of DNA synthesis up to 400 μM TTP (data not shown), as has been observed previously by Wang et al. (*17*) using homopolymer templates. Therefore, Mn^{2+} was used as the catalytic ion in all kinetic analyses, as previously described by others for comparisons of β-wt and mutants in assays using homopolymer templates (*14*, *18*).

Initial velocities for gap filling DNA synthesis were determined for each polymerase from reaction plots of product versus time. Typical reaction progress curves for pol β-wt are shown in Figure 2A. The reaction rate decreased during the assay for all enzymes examined. This decrease was not due to limiting DNA template [K_m(DNA) < 300 nM; data not shown] but rather to inactivation or trapping of the enzyme during the reaction.

Primer extension analysis was used to characterize gap filling by pol β-wt under the conditions and template:enzyme ratios in the kinetic analyses, with either $MgCl_2$ or $MnCl_2$ (panels A and B of Figure 3, respectively). The control templates contained a 5′OH at the gap terminus which eliminates pol β binding via the 8 kDa domain to this moiety (*19*). The DNA product distribution from the primer extension reactions was analyzed by computer simulation using the model shown in Scheme 1 (see Materials and Methods). The model yields a predicted product distribution similar to that observed in Figure 3 on both experimental (5′PO_4) and control (5′OH) templates. Simulated mechanisms of activity loss by enzyme inactivation or trapping yielded equivalent results. In addition to gap-filled products, we observed products representing extension beyond the gap on the 5′PO_4 templates for both cations (Figure 3). The product distribution and the model in Scheme 1 indicate that the rate of incorporation and substrate affinity was altered at the gap terminus compared to prior incorporations [Mg^{2+} (k_3/k_7 = 11) and Mn^{2+} (k_3/k_7 = 20)], consistent with an altered mechanism. Products greater than five nucleotides represent either displacement of the downstream primer and TMP misincorporation opposite template G or primer misalignment resulting in TMP base additions. Since this alteration in the reaction pathway occurs at the gap terminus, it does not affect the initial velocity, although it may contribute to the observed decrease in reaction rate during the kinetic assay (Figure 2A). However, the presence of products extended beyond the gap terminus precludes analysis of the fidelity of DNA synthesis in small gapped templates via the HSV-*tk* forward mutation assay (see below). Interpretation of results obtained in the HSV-*tk* assay depends on the assumption that there is a one-to-one correspondence between the observed mutation frequency and the frequency of DNA polymerase errors (*15*). This assumption may be invalid using gapped templates, as the strand displacement products create flap structures which cannot be ligated efficiently and which might be processed aberrantly after transfection into *E. coli*. Moreover, we have observed that the amount of strand-displaced products is greater under nonlimiting enzyme conditions and is greater for some of the Y265 variant polymerases, relative to wild-type (data not shown).

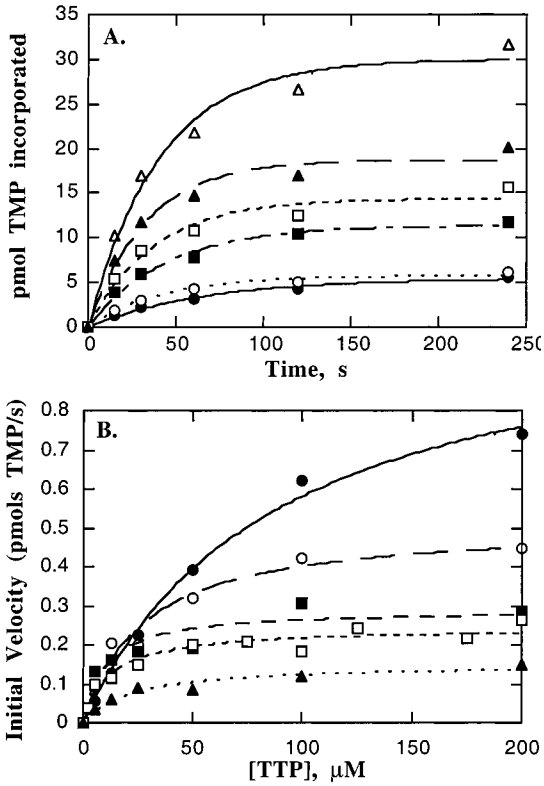

FIGURE 2: Steady-state kinetic analyses of pol β-wt and Y265 substitutions. (A) Effect of [dTTP] on pol β-wt reaction rates. Reactions contained 20 nM pol β-wt and either 5 μM (●), 12.5 μM (○), 25 μM (■), 50 μM (□), 100 μM (▲), or 200 μM (△) TTP. Curves were fit to the equation describing a first-order decay, $y = c(1 - e^{-bt})$, and initial velocity was determined by solving the first derivative of the equation for time = 0. (B) Initial velocity versus substrate concentration for Y265 substitutions. A representative plot of initial velocity versus nucleotide substrate concentration is shown for each polymerase and was fit to the Michaelis−Menten equation. Reactions contained either 20 nM β-wt (●), 20 nM Y265F (○), 20−40 nM Y265W (■), 40 nM Y265L (□), or 60 nM Y265S (▲).

Effect of Y265 Substitutions on the Kinetics of DNA Synthesis. Plots of initial velocities versus TTP concentration were hyperbolic and fit to the Michaelis−Menten equation (Figure 2B). The Michaelis−Menten constants K_m(TTP) and k_{cat} for pol β-wt and the Y265 substitutions are shown in Table 1. Interestingly, all substitutions displayed lower k_{cat} values, relative to β-wt, in the following order of decreasing magnitude: β-wt > Y265F > Y265W > Y265L > Y265S (Table 1). The K_m(TTP) values of Y265F, Y265S, and

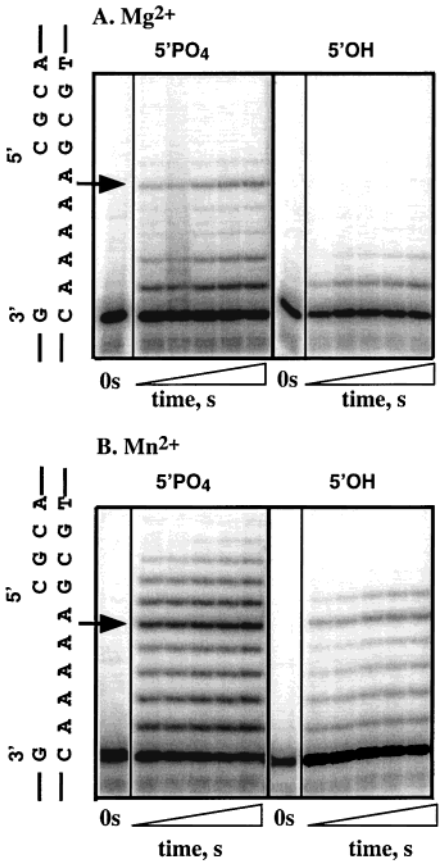

FIGURE 3: Primer extension products for polymerase β-wt in the kinetic assay. DNA-gapped templates contained either a 5′-phosphorylated (5′PO_4) or nonphosphorylated (5′OH) downstream oligonucleotide. Phosphorimager scans are of DNA synthesis products separated on a 16% polyacrylamide gel for reactions containing 100 μM TTP, 6.7 nM pol β-wt, either 10 mM $MgCl_2$ (A) or 2 mM $MnCl_2$ (B), and either 100 nM (5′PO_4) gapped template (from left, lanes 1−6) or 100 nM (5′OH) control template (lanes 7−12); arrows indicate the gap terminus. Reactions were incubated at 37 °C in reaction buffer, and aliquots were removed at 5, 30, 60, 120, and 240 s. The total percent of primers extended in each reaction after 240 s is as follows: for Mg^{2+} (A), 27.3% for 5′PO_4 and 15.2% for 5′OH templates; for Mn^{2+} (B), 51.2% for 5′PO_4 and 24.3% for 5′OH templates.

Table 1: Michaelis−Menten Constants for Pol β-wt and Y265 Substitutions[a]

	K_m(TTP) (μM)		k_{cat} (s^{-1})		k_{cat}/K_m
polymerase	average	range	average	range	($M^{-1}\,s^{-1}$)
Y265 wt	84	79−88 (2)	1.8	1.7−1.8 (2)	2.1×10^4
Y265F	28	27−29 (2)	0.92	1.0−0.85 (2)	3.3×10^4
Y265W	9.0	6.2−11 (3)	0.35	0.30−0.51 (3)	3.9×10^4
Y265L	15	13−18 (2)	0.28	0.20−0.34 (2)	1.9×10^4
Y265S[b]	22	na[c]	0.083	na	3.8×10^3

[a] The number of independent determinations is given in parentheses. Catalytic efficiency (k_{cat}/K_m) was calculated from the average values for K_m(TTP) and k_{cat} for each polymerase. [b] Single determination. [c] na: not available.

Y265L were 3−6-fold lower than that of β-wt, while the value for Y265W was decreased 9-fold (Table 1). Consequently, mutant polymerases Y265F, Y265W, and Y265L displayed catalytic efficiencies [k_{cat}/K_m(TTP)] similar to that of wild type. In contrast, the Y265S substitution was compromised for DNA synthesis activity: catalytic efficiency was 6-fold lower than for wild type, and the catalytic rate constant was reduced 22-fold lower (Table 1).

Table 2: HSV-*tk* Mutation Frequencies $\times 10^{-4}$ for Pol β-wt and Y265 Substitutions[a]

polymerase	10 mM $MgCl_2$	2 mM $MnCl_2$
Y265 wt	32 ± 7.7	43
Y265F	35 ± 15	42
Y265W	260 ± 45	100
Y265L	260 ± 45	120
Y265C	730 ± 200	580
Y265S[b]	1300 ± 500	620

[a] The HSV-*tk* mutation frequencies for reactions containing 10 mM $MgCl_2$ represent the mean ± standard deviations from three to four independent reactions. [b] The Y265S values are from reactions that yielded approximately 2-fold less synthesis than other clones, due to significantly decreased catalytic activity.

Effect of Y265 Substitutions on DNA Synthesis Fidelity. To determine the fidelity of DNA synthesis for the Y265 substitutions, relative to β-wt, we tested each polymerase in the HSV-*tk* forward mutation assay. The relative protein levels needed to achieve nearly equivalent amounts of DNA synthesis among the polymerases agreed well with the relative catalytic efficiencies of the polymerases obtained under steady-state conditions (Table 1 and data not shown). Due to the low catalytic efficiency of the Y265S substitution, the maximal amount of this enzyme that could be added to the reaction yielded about 2.6-fold less synthesis than wild type (data not shown). However, the HSV-*tk* mutation frequency is not dependent on total DNA synthesis levels; we observed that various pol β-wt amounts (0.5−3.6 μM) yielded identical mutation frequencies (K. Eckert, unpublished data).

HSV-*tk* mutation frequencies, which are an estimate of the polymerase error frequency during in vitro DNA synthesis, were determined for each polymerase from three to four independent reactions, as previously described (*4*, *15*) (Table 2). The values for histidine-tagged pol β-wt and Y265C agree well with previous results obtained using proteins purified via maltose tags [$(21 \pm 5.4) \times 10^{-4}$ and $(540 \pm 76) \times 10^{-4}$, respectively (*3*)] and with recombinant pol β-wt lacking a purification tag [$(24 \pm 7.0) \times 10^{-4}$ (*15*)]. Among the mutant polymerases examined, only the Y265F polymerase retained a wild-type mutation frequency (Table 2). Interestingly, both hydrophobic substitutions, Y265L and Y265W, displayed equivalent mutator phenotypes in the presence of $MgCl_2$ (8-fold above β-wt) (Table 2). The polar substitutions, Y265C and Y265S, displayed the most severe effect on fidelity (23-fold and 41-fold, respectively). HSV-*tk* mutation frequencies also were determined using 2 mM $MnCl_2$ for comparison with the kinetic data. Interestingly, the mutation frequencies for pol β-wt and Y265F were not altered significantly relative to Mg^{2+}. However, the mutation frequency for each mutator was decreased relative to Mg^{2+} values. Importantly, we found that altering the catalytic ion did not alter the relative order of mutator effects displayed by the 265 substitutions. With either Mg^{2+} or Mn^{2+} as the catalytic ion, polymerase Y265F retained a wild-type mutation frequency, while Y265W and Y265L were intermediate mutators, and Y265C and Y265S were the strongest mutators.

To determine polymerase error specificities, independent polymerase-induced HSV-*tk* mutants were sequenced from reactions containing either polymerase Y265F, Y265W, or Y265L (Tables 3 and 4 and Figure 4). Polymerase Y265S

Table 3: HSV-*tk* Mutants Containing Deletions and Multiple Mutations for Y265W and Y265L

mutant class	Y265W	Y265L
single mutation, large deletions[a]	111−118 △8 bp	183−187 △5 bp
	225−238 △14 bp (2)	240−269 △30 bp
	240−268 △29 bp	241−267 △27 bp
	240−269 △30 bp (2)	241−268 △28 bp
	241−269 △29 bp (2)	242−268 △27 bp
two mutations[b]	95 T→C, 247 A→C*	95 T→C, 247 A→C*
	112 T→G, 225−238 △14 bp	91 G→A, 227 C→G*
	119 G→A, 226−229 △C	[106−110 ◊GC, 111 T→G]
	146 G→A, 221 A→G*	[107 C→T, 111−112 ▲C]
	146 G→A, 209 G→A*	146 G→T, 226−229 ▲C
	146 G→A, 238 G→A*	169 A→G, 272 △T
	148−149 ◊C, 182 C→T	213 T→G, 273−275 △G
	157 C→T, 229 C→T*	[237−240 ▲G, 241−269 △29 bp]
	199−200 ◊AC, 281 G→A	[277 T→C, 277−278 ▲G]
	[244−245 C→T, 244−245 △*C*]	
	226−229 ▲C, 236 T→C	
three to five mutations[b]	[111 T→G, 121−146 △26 bp]	[252 G→A, 253 △A]
	157 C→T	212−214 △T
	236 T→C, 251−252 △C	[273−275 △G, 278 C→T]
	279 G→C	111 T→G, 156 G→A
		237−240 ▲G

[a] Deletion of >2 bases. The number of independent mutants observed is shown in parentheses. [b] Changes in brackets denote tandem or near tandem errors. Detectable base substitutions are indicated by an asterisk. Frame shifts: one-base deletions (△), one-base additions (▲), and two-base deletions (◊).

was not analyzed further due to the low activity of this enzyme. An increase in the frequency of multiple polymerase-induced mutations observed in the 203 base pair HSV-*tk* target was observed for polymerases Y265W (58×10^{-4}) and Y265L (67×10^{-4}) but not for Y265F (1.3×10^{-4}), compared to β-wt [0.49×10^{-4} (*4*)]. However, the increase in multiple mutations was less severe for Y265W and Y265L than was observed previously for Y265C (*4*). The specificity of multiple mutations produced by polymerases Y265F, Y265W, and Y265L is shown in Table 3. The observed HSV-*tk* mutation frequencies were corrected for the existence of multiple mutations by determining the total number of independent, detectable polymerase errors, to calculate polymerase estimated error frequencies (Table 4) (*4*). The error frequencies were used to calculate the frequencies of detectable base substitutions, frame shifts, large deletions, and tandem errors within the mutagenic target. All pol β Y265 substitutions retained the wild-type pol β characteristic of producing more frame-shift errors than base substitution errors in the target sequence (Table 4). Again, Y265F appeared wild type in error frequencies and specificities. Polymerases Y265W and Y265L were similar to each other and to Y265C in that all three are general mutators and display a nearly equivalent increase in base substitutions (18-fold Y265W and Y265L) and frame-shift errors (15-fold Y265W, 14-fold Y265L) relative to pol β-wt. Overall, Y265W and Y265L substitutions share similar error frequencies and error specificities and describe an intermediate mutator effect, falling between the Y265F and Y265C substitutions.

Effect of Substitutions Y265F, Y265W, and Y265L on Frame-Shift Errors. Interestingly, the hot spots in the target sequence for one-base deletion and insertion errors are relatively constant among the various polymerases (Figure 4). The majority of one-base deletion and insertion errors for all polymerases occurred in homonucleotide sequences, consistent with a misalignment mechanism of frame-shift production. The previously described hot spot for minus two base errors by pol β-wt (*4*), a dinucleotide $(TA)_3$ (214−219) sequence, was also observed for Y265F but not for the mutators Y265C (*4*), Y265W, and Y265L. The difference in the proportion of two-base deletions at this site, relative to pol β-wt [22/87 (*4*)], is not significant for Y265F (4/35). However, the number of occurrences for Y265W (1/58) is significantly lower than for pol β-wt ($p = 0.0006$), while no errors at this site were observed for Y265L. Furthermore, while the mutator Y265W displays increased frame-shift errors in general, the frequency of two-base deletions at the $(TA)_3$ (214−219) sequence for Y265W (4.5×10^{-4}) is not greater than for β-wt [3.5×10^{-4} (*4*)] or Y265F (2.6×10^{-4}). Thus, the mutators Y265W, Y265L, and Y265C do not share the strong two-base deletion error hot spot observed for the wild-type and Y265F enzymes, suggesting differences in polymerase interactions with the template.

Polymerases Y265W and Y265L Alter the Frequency of Large Deletion Errors. The Y265W and Y265L alterations increased the frequency of large deletion errors (greater than two nucleotides deleted) relative to wild type (83-fold and 67-fold, respectively), whereas the Y265C mutator increased the frequency of these errors only 21-fold (Table 4). No increase in large deletion errors was observed for the Y265F polymerase relative to β-wt. To ensure that the observed increases in large deletion errors were not an artifact due to the alternative procedure used to purify the proteins (his-tag versus maltose-tag method), we sequenced HSV-*tk* mutants from a representative reaction using his-tag purified β-wt. We observed a large deletion frequency of 2.1×10^{-4}, and the proportion of these errors (2/27) is not significantly different from the value observed for the previously reported rat pol β-wt [3/86 (*4*)]. Li et al. (*13*), using a variation of the HSV-*tk* assay, observed a similar frequency of large deletion errors (0.85×10^{-4}). Thus, the Y265W and Y265L polymerases are not only general mutators for frame-shift and base substitution errors but also specific mutators for large deletion errors.

DISCUSSION

In this study, we tested the hypothesis that both the hydrophobic and van der Waals contacts tyrosine 265 of polymerase β makes with neighboring residues in the hinge region are critical for DNA synthesis activity and fidelity. Consistent with the importance of hydrophobicity in this region, we found that phenylalanine, leucine, and tryptophan substitutions did not significantly alter the steady-state catalytic efficiency relative to wild type, while serine compromised catalytic efficiency (Table 1). Hydrophobic interactions of residue 265 in the hinge appear to be necessary for fidelity, given that the mutator effect for the tryptophan and leucine substitutions was intermediate compared to substitution of the more polar side chains of cysteine and serine. However, we found that maintenance of both the hydrophobicity and van der Waals volume of residue 265 is not sufficient for maintaining fidelity of DNA synthesis (Tables 2 and 4).

Table 4: Error Specificities for Pol β-wt and Y265 Substitutions

	frequency $\times 10^{-4}$ (no. of detectable, independent errors)				
error type	Y265 wt[a]	Y265F	Y265W	Y265L	Y265C[a]
estimated error frequency[b]	14	23	260	270	470
detectable base substitutions	3.2 (20)	6.6 (10)	58 (13)	58 (9)	74 (14)
frame shifts	10 (63)	16 (25)	150 (34)	140 (22)	330 (63)
large deletions	0.48 (3)	<0.66	40 (9)	32 (5)	10 (2)
complex, tandem errors[c]	0.16 (1)	<0.66	9.0 (2)	38 (6)	48 (10)
no. of independent polymerase errors	87	35	58	42	89

[a] Values are from reactions using the maltose-tag clones (*4*). [b] Obtained by correcting the MF_{obs} for mutants with multiple errors (see Materials and Methods). MF_{obs} for Y265F, Y265W, and Y265L was 24×10^{-4}, 260×10^{-4}, and 260×10^{-4}, respectively. [c] Adjacent or closely spaced multiple HSV-*tk* mutations that are considered to result from a single polymerase error event.

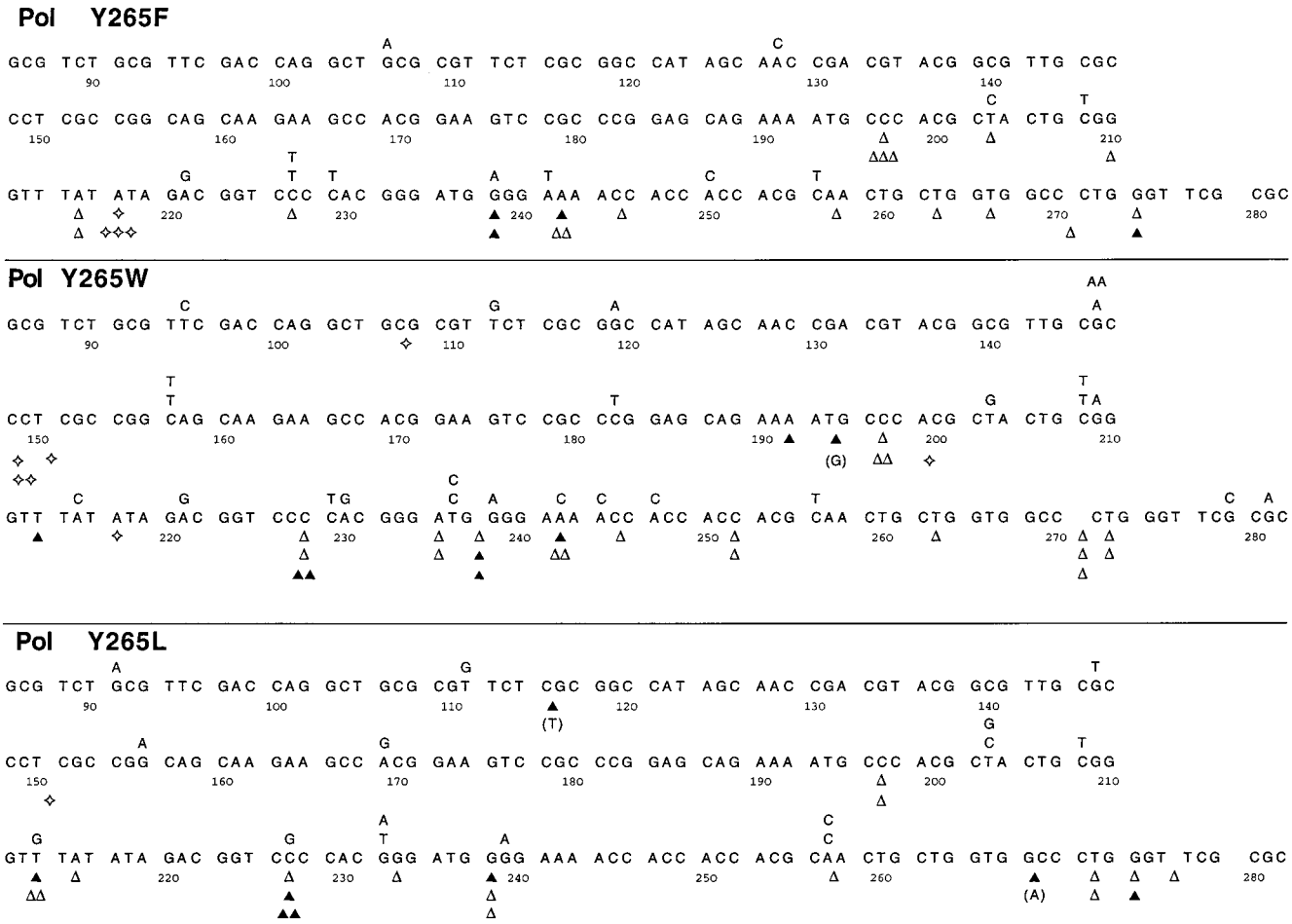

FIGURE 4: HSV-*tk* forward mutational specificity of polymerases Y265F, Y265W, and Y265L. The DNA template shown is the *Mlu*I−*Eco*RV mutagenic target. Letters above the line indicate base substitutions, and symbols below the line represent frame-shift mutations: one-base deletions (△), one-base additions (▲), and two-base deletions (◇). Tandem multiple mutations were excluded (Table 3). Two HSV-*tk* mutants containing multiple mutations resulted from reactions with polymerase Y265F: (1) 106 G→A and 196−198 ΔC; (2) 128 A→C and 214−219 GTA.

Role of Tyrosine 265 in Catalytic Efficiency. Substitution of a polar serine residue [side chain hydropathy = 1.24 kcal/mol (*10*)] results in a nearly 6-fold reduction in catalytic efficiency, and a 22-fold reduction in the catalytic rate constant, relative to β-wt (Table 1). The polar-like cysteine [hydropathy = −0.20 kcal/mol (*10*)] substitution was also reported to compromise catalysis, as indicated by a 20-fold decrease in catalytic rate constant relative to β-wt (*3*). In contrast, the hydrophobic substitutions of F, L, and W display an equivalent or greater catalytic efficiency than β-wt [hydropathy: Y = −1.47, F = −2.27, L = −1.82, and W = −2.13 kcal/mol (*10*)]. We postulate that the hydrophobic contacts that Y265 makes with neighboring residues are required for proper hinge mediation of the conformational change during normal catalysis.

Role of Tyrosine 265 in Fidelity. The X-ray crystal structure describes the hinge region of pol β as lined by hydrophobic residues and a number of equally favorable interactions in both the open and closed conformations (*5*, *8*) (Figure 1). The transition from open to closed upon binding dNTP residues is predicted to play an important role in fidelity of DNA synthesis by an induced fit mechanism that discriminates against mispairs and misaligned primer/templates (reviewed in refs *1* and *2*). The Y265S and Y265C polar substitutions most clearly demonstrate the importance of the hinge hydrophobic interactions in maintaining the

fidelity of DNA synthesis (Table 2). However, maintenance of hydrophobicity was not sufficient for retaining a wild-type phenotype, as the Y265W and Y265L hydrophobic substitutions displayed increased HSV-*tk* error frequencies relative to β-wt (Table 2). While leucine and phenylalanine share similar van der Waals volume with tyrosine [Y = 141 Å^3, F = 135 Å^3, and L = 124 Å^3 (*9*)], phenylalanine was the only other amino acid at position 265 examined thus far which retains wild-type fidelity. Thus, our data show that additional interactions between residue 265 and neighboring residues must function in fidelity and suggest the requirement of an aromatic ring structure. In the pol β closed conformation, the tyrosine 265 aromatic ring stacks in a perpendicular fashion with the aromatic ring of tyrosine 266 (Figure 1) (*5*). The negative charge above and below an aromatic ring, due to π electrons, can form electrostatic interactions with the positively charged plane (edge) of a perpendicular neighboring aromatic ring (*20*).

We found the exquisite sensitivity of pol β error rates to the nature of the residue at position 265 surprising, given that this residue is predicted to be removed from the active site (*5*). A survey of 26 Klenow polymerase mutants near the active site revealed that only five alterations resulted in a mutator phenotype (*21*), while a screen of pol β mutants identified mutators at a frequency of only 1 in 100 (*3*). Both studies suggest that polymerase fidelity may not be easily perturbed. Furthermore, all of the pol β Y265 substitution mutators identified and examined thus far at position 265 are general mutators and display a nearly equivalent increase in both misalignment-initiated frame-shift (~14−33-fold) and misincorporation-initiated base substitution errors (~18−23-fold). To our knowledge, the only other mutators described that display an increase in both types of errors is Klenow R682A [3-fold for base substitutions and 1.6-fold for frame shifts, relative to wild type (*21*)] and pol β mutator F272L (*13*). A distinguishing feature of the Y265W and Y265L error specificity is a 67−83-fold increase in the frequency of large deletions relative to β-wt. These large deletions occurred to a lesser extent in the Y265C error spectrum (*4*). Because deletions in the β-wt, Y265W, Y265L, and Y265C spectra arise in the same sequence context (Table 3 and ref *4*), we assume they are produced by similar mechanisms. The deletions can be explained by the formation of hairpins (*22*) at specific sites within the HSV-*tk* sequence. The Y265L and Y265W substitutions may alter the DNA binding constant of the polymerase and/or the processivity of the enzyme, causing a higher probability of dissociation when approaching the hairpin relative to β-wt, thus favoring deletion formation.

Model for Increased Error Production by Y265 Substitutions. Substitution at position 265 potentially decreases the pol β discrimination parameters at the levels of (1) the stability of the pol β·DNA·dNTP intermediate complex and/or (2) the rate of the conformational change. Although Y265 does not contact either substrate, substitutions at this residue may indirectly affect the stability and/or binding affinity for dNTPs by perturbing the geometry of the active site and shifting the position of critical residues. The X-ray crystal structures describe F272 as a hydrophobic residue interacting in the hinge domain (*8*) (Figure 1), and Li et al. (*13*) found that this residue functions in nucleotide discrimination at the level of binding. Alternatively, Y265 substitutions may perturb the polymerase to allow general water access to the active site which could stabilize premutagenic intermediates (*23*). Perhaps polar substitutions at 265 allow greater or more frequent water access than hydrophobic substitutions.

The Y265 alterations may also affect the rate of the conformational change that is predicted to play an important role in fidelity and that is normally rate limiting (*5*, *7*). Perturbing of the hinge region could disrupt the interactions that stabilize the open and/or closed conformations (*5*, *8*), thus altering the rate of conformational change. For example, upon formation of the closed structure F272 shifts position and breaks a salt bridge between R258 and D192, thereby freeing D192 to coordinate with the nucleotide (*5*). Alternatively, pol β may form an aberrant, error-tolerant closed conformation during misincorporation, given predictions that mispairs cause steric hindrance in the closed conformation active site (*5*). A slower rate of conformational change to the error-tolerant state, relative to the correct state, would ensure large rate differences between incorporation of correct and incorrect nucleotides, as has been observed (*7*). Y265 substitutions may increase the formation rate of this error-tolerant state, thereby shrinking discrimination via rate differences.

In summary, substitution at residue 265 of polymerase β resulted in three classes of enzyme: (1) wild-type activity and fidelity, Y and F; (2) wild-type activity and moderately decreased fidelity, W and L; and (3) decreased activity and greatly decreased fidelity, C and S. Given this observed differential effect, we propose that the relative impact of 265 substitutions on either discrimination parameter, nucleotide binding affinity/stability or conformational change rate, is determined by the specificity of residue 265 interactions in the hinge domain. Given the role of polymerase β in repair of DNA damage, the accuracy of DNA repair synthesis by polymerase β is important in nonmitotic cell populations. The error-prone polymerase β, Y265C, has been shown to increase the spontaneous cellular mutation frequency in a dominant negative fashion when expressed in *Saccharomyces cerevisiae* and in LN12 mouse cells (*24*, *25*). Our studies demonstrate that a single amino acid substitution can produce a mutator form of a DNA polymerase that retains full catalytic efficiency, providing in vitro evidence to support the principle that mutations in DNA polymerase genes can contribute to genomic instability without compromising normal DNA metabolic activities.

ACKNOWLEDGMENT

We thank Guang Yan for technical support. We are grateful to Suzanne Hile and Drs. William A. Beard, Katarzyna Bebenek, Thomas A. Kunkel, Vineeta Khare, and Joann B. Sweasy for critical reading of the manuscript. We also gratefully acknowledge the generous contributions made to The Jake Gittlen Cancer Research Institute.

REFERENCES

1. Kunkel, T. A., and Wilson, S. H. (1998) *Nat. Struct. Biol. 5*, 95−99.
2. Goodman, M. F. (1997) *Proc. Natl. Acad. Sci. U.S.A. 94*, 10493−10495.
3. Washington, S. L., Yoon, M. S., Chagovetz, A. M., Li, S.-X., Clairmont, C. A., Preston, B. D., Eckert, K. A., and Sweasy, J. B. (1997) *Proc. Natl. Acad. Sci. U.S.A. 94*, 1321−1326.

4. Opresko, P. L., Sweasy, J. B., and Eckert, K. A. (1998) *Biochemistry 37*, 2111−2119.
5. Sawaya, M. R., Prasad, R., Wilson, S. H., Kraut, J., and Pelletier, H. (1997) *Biochemistry 36*, 11205−11215.
6. Werneburg, B. G., Ahn, J., Zhong, X., Hondal, R. J., Kraynov, V. S., and Tsai, M.-D. (1996) *Biochemistry 35*, 7041−7050.
7. Zhong, X., Patel, S. S., Werneburg, B. G., and Tsai, M.-D. (1997) *Biochemistry 36*, 11891−11900.
8. Pelletier, H., Sawaya, M. R., Wolfle, W., Wilson, S. H., and Kraut, J. (1996) *Biochemistry 35*, 12742−12761.
9. Creighton, T. E. (1993) *Protein Structures and Molecular Properties*, 2nd ed., W. H. Freeman and Co., New York.
10. Roseman, M. A. (1988) *J. Mol. Biol. 200*, 513−522.
11. Kunkel, T. A., Bebenek, K., and McClary, J. (1991) *Methods Enzymol. 204*, 125−139.
12. Kosa, J. L., and Sweasy, J. B. (1999) *J. Biol. Chem. 274*, 3851−3858.
13. Li, S.-X., Vaccaro, J. A., and Sweasy, J. B. (1999) *Biochemistry 38*, 4800−4808.
14. Menge, K. L., Hostomsky, Z., Nodes, B. R., Hudson, G. O., Rahmati, S., Moomaw, E. W., Almassy, R. J., and Hostomska, Z. (1995) *Biochemistry 34*, 15934−15942.
15. Eckert, K. A., Hile, S. E., and Vargo, P. L. (1997) *Nucleic Acids Res. 25*, 1450−1457.
16. Rosner, B. (1995) *Fundamentals of Biostatistics*, Wadsworth Publishing Co., Belmont, CA.
17. Wang, T. S.-F., Eichler, D. C., and Korn, D. (1977) *Biochemistry 16*, 4927−4934.
18. Beard, W. A., Osheroff, W. P., Prasad, R., Sawaya, M. R., Jaju, M., Wood, T. G., Kraut, J., Kunkel, T. A., and Wilson, S. H. (1996) *J. Biol. Chem. 271*, 12141−12144.
19. Prasad, R., Beard, W. A., and Wilson, S. H. (1994) *J. Biol. Chem. 269*, 18096−18101.
20. Hunter, C. A., Singh, J., and Thornton, J. M. (1991) *J. Mol. Biol. 218*, 837−846.
21. Minnick, D. T., Bebenek, K., Osheroff, W., Turner, R. M., Jr., Astatke, M., Liu, L., Kunkel, T. A., and Joyce, C. M. (1999) *J. Biol. Chem. 274*, 3067−3075.
22. Ripley, L. S. (1990) *Annu. Rev. Genet. 24*, 189−213.
23. Petruska, J., Goodman, M. F., Boosalis, M. S., Sowers, L. C., Cheong, C., and Tinoco, I., Jr. (1988) *Proc. Natl. Acad. Sci. U.S.A. 85*.
24. Clairmont, C. A., and Sweasy, J. B. (1998) *J. Bacteriol. 180*, 2292−2297.
25. Clairmont, C. A., Narayanan, L., Sun, K.-W., Glazer, P. M., and Sweasy, J. B. (1999) *Proc. Natl. Acad. Sci. U.S.A. 96*, 9580−9585.

BI000698T